J Mater Sci (2008) 43:4693–4700
DOI 10.1007/s10853-007-2420-1

REACTIVITY OF SOLIDS

The role of protons in ionic diffusion in (Mg, Fe)O and $(Mg, Fe)_2SiO_4$

David L. Kohlstedt · Stephen J. Mackwell

Received: 31 October 2007 / Accepted: 20 December 2007 / Published online: 30 April 2008

Abstract The presence of hydrogen dissolved within iron-magnesium oxides and silicates results in an increase in the rate of Fe–Mg interdiffusion. Experimental data and point defect models suggest that the increased interdiffusivity is due to an increase in the total metal-vacancy concentration through stabilization of proton-vacancy defect associates in a hydrous environment. In the case of $(Mg_{1-x}Fe_x)O$, interdiffusion experiments under hydrothermal conditions at a fluid pressure of $\sim$0.3 GPa yield similar dependencies of interdiffusivity on Fe-content, oxygen fugacity, and temperature as under dry conditions, but interdiffusion coefficients are a factor of $\sim$3 larger. These data suggest that the increased interdiffusivities in $(Mg_{1-x}Fe_x)O$ result from incorporation of defect associates formed between a metal vacancy and a single proton, $p'_{Me} \equiv \{p^{\bullet} - V''_{Me}\}'$. For $(Mg_{1-x}Fe_x)_2SiO_4$, interdiffusion under hydrothermal conditions over a range of fluid pressures reveals a significant difference in the dependence of interdiffusivity on Fe content than obtained under dry conditions, combined with a strong dependence on water fugacity. These data indicate that the increased diffusivities in $(Mg_{1-x}Fe_x)_2SiO_4$ result from incorporation of defect associates involving a metal vacancy and 2 protons, $(2p)^{\times}_{Me} \equiv \{2p^{\bullet} - V''_{Me}\}^{\times}$. It is anticipated that, at higher water fugacities, Fe–Mg interdiffusion in both materials will become dominated by these latter defects and that the interdiffusivity will increase linearly with water fugacity but will be independent of oxygen fugacity and iron concentration.

D. L. Kohlstedt (✉)
Department of Geology and Geophysics, University of Minnesota, Minneapolis, MN 55455, USA
e-mail: dlkohl@umn.edu

S. J. Mackwell
Lunar and Planetary Institute, 3600 Bay Area Boulevard, Houston, TX 77058, USA

Introduction

In the 1960s, earth scientists became keenly aware of the importance of a small concentration of protons on the kinetic properties of nominally anhydrous minerals,[1] NAMs [for reviews, see 1–3]. High-pressure, high-temperature creep experiments on quartz and olivine—SiO_2 and $(Mg, Fe)_2SiO_4$—revealed a dramatic weakening if samples were deformed in a hydrous environment rather than under anhydrous conditions [4, 5]. This phenomenon was immediately termed 'water weakening' or 'hydrolytic weakening,' the former reflecting the availability of water in the deformation assembly and the latter indicating the detection of OH (hydroxyl) stretching bands in infrared analyses performed on deformed samples. Subsequent studies recognized the importance of protons in this weakening phenomenon since H^+ ions—that is, protons—are charged [6, 7] and diffuse extremely rapidly [8, 9]. Trace amounts of protons are also correlated with weakening of other nominally anhydrous silicate minerals including plagioclase, $(Na, Ca)Al_2Si_2O_8$ [e.g., 10] and clinopyroxene, $(Mg, Ca)SiO_3$ [e.g., 11, 12].

Over the past decade, investigators have taken research on the effect of protons on kinetic properties in a more quantitative direction. While early experiments focused on the difference between the behavior of a mineral in a hydrous environment versus its behavior under anhydrous conditions, current experiments emphasize the dependence

[1] A nominally anhydrous mineral is one in which hydrogen ions are not part of the regular structure but rather exist as point defects.

of a specific property on proton concentration [13–21]. Furthermore, experiments now include not only high-temperature deformation but also ionic diffusion [22–24] and electrical conductivity [25–27].

Since experiments in the earth sciences are generally undertaken to investigate the properties of minerals and rocks that occur at depth, a common approach in many laboratories involves the use of high-pressure, high-temperature testing equipment. In the context of studies on the role of protons on kinetic properties, the concentration of hydrogen ions or protons, C_H, in a nominally anhydrous mineral such as magnesiowüstite, $(Mg_{1-x}Fe_x)O$, or olivine, $(Mg_{1-x}Fe_x)_2SiO_4$, can be described by the relation

$$C_H = A f_{H_2O}^m f_{O_2}^n a_{MeO}^q x^r \exp\left(-\frac{E+PV}{RT}\right) \quad (1)$$

where A is a material-dependent parameter, f_{H_2O} is water fugacity, f_{O_2} is oxygen fugacity, a_{MeO} is activity of metal oxide, and x is the fraction of iron in metal sites, Me = Mg + Fe. In Eq. 1 E and V are the activation energy and activation volume for incorporation of protons in the crystal structure, P is the confining pressure, and RT has the usual meaning. It should be noted that for an oxide $a_{MeO} \approx 1$. Based on Eq. 1, pressure affects the concentration of hydrogen in two ways. First, it influences the concentration of hydrogen directly through the pressure-volume term that appears in the exponential function; if $V > 0$, then C_H decreases with increasing pressure. Second, pressure affects the concentration of hydrogen indirectly through its effect on water fugacity; based on the equation of state for water [28], water fugacity increases with increasing pressure in the manner illustrated in Fig. 1.

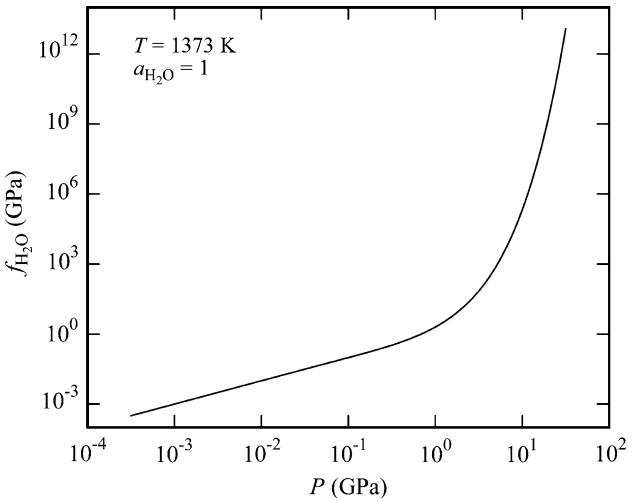

Fig. 1 Plot of water fugacity as a function of pressure at $T = 1{,}373$ K for water activity equal to unity, $a_{H_2O} = 1$, that is, for pure water. In reality, all minerals are soluble to some degree in a hydrous fluid, thus somewhat lowering the water activity

In this article, we examine the role of protons on ionic diffusion in olivine, the primary mineral in Earth's upper mantle, and in magnesiowüstite (also referred to as ferropericlase), the second most abundant mineral in the lower mantle. We start by reviewing point defect thermodynamics for (Mg, Fe)-oxides and (Mg, Fe)-silicates. We then extend our analyses to Mg–Fe interdiffusion in these two systems. For (Mg, Fe)O, for which interdiffusion data are available over a range of temperatures at a single pressure, we normalize all data to a common oxygen fugacity. This approach permits a reassessment of the charge neutrality condition as well as the cause of the enhancement in interdiffusivity associated with the presence of protons. For $(Mg, Fe)_2SiO_4$, for which interdiffusion data are available over a range of pressures and, thus, water fugacity at a single temperature, we examine the dependence of interdiffusivity on iron concentration. Through this analysis and an examination of point defect models describing metal-vacancy concentration as a function of water fugacity, oxygen fugacity, and iron concentration, we are able to identify the dominant source of cation vacancies that facilitates the substantial increase in interdiffusivity due to the addition of protons. Characterization of the role of hydrogen on kinetic properties is important in earth sciences as hydrogen is the most abundant element in the universe and is ubiquitous throughout the interiors of Earth and other planets.

Point defect thermodynamics

Under anhydrous conditions, the majority of point defects are normally $Fe_{Me}^{\bullet}$ and V_{Me}'' for both (Mg,Fe)O [29, 30] and $(Mg, Fe)_2SiO_4$ [9, 31] with charge neutrality given by

$$[Fe_{Me}^{\bullet}] = 2[V_{Me}''] . \quad (2)$$

Here, we use the Kröger–Vink notation [32] to indicate species (A), defect site (s), and defect charge (c) as A_s^c. With the application of the law of mass action to the usual reaction involving $Fe_{Me}^{\bullet}$ and V_{Me}'',

$$\frac{1}{2}O_2 + 2Fe_{Me}^{\times} + Me_{Me}^{\times} \Leftrightarrow 2Fe_{Me}^{\bullet} + V_{Me}'' + MeO(srg), \quad (3)$$

we obtain the relation

$$K_3[Fe_{Me}^{\times}]^2 f_{O_2}^{1/2} = [Fe_{Me}^{\bullet}]^2[V_{Me}'']a_{MeO}, \quad (4)$$

where *srg* indicates a site of repeatable growth and K_3 is the equilibrium constant for reaction (3). To arrive at Eq. 4, $[Me_{Me}^{\times}]$ was approximated as unity. For charge neutrality defined by Eq. 2, Eq. 4 becomes

$$[Fe_{Me}^{\bullet}] = 2[V_{Me}''] \propto f_{O_2}^{1/6}[Fe_{Me}^{\times}]^{2/3} a_{MeO}^{-1/3} . \quad (5)$$

While a_{MeO} is approximately unity in (Mg, Fe)O, it will generally be less than unity for $(Mg, Fe)_2SiO_4$ in Earth's

upper mantle, where olivine-rich rocks are buffered by the presence of orthopyroxene, (Mg, Fe)SiO_3. The dependencies of the concentrations of several point defects on oxygen fugacity, water fugacity, activity of MeO, and iron content are given for several charge neutrality conditions in Table 1 for both anhydrous and hydrous conditions.

Under hydrous conditions, protons can be incorporated as either positively or negatively charged point defects. A variety of charge neutrality conditions involving protons, $p^\bullet$, are possible, including

$$[p^\bullet] = 2[V''_{Me}], \tag{6a}$$

$$[Fe^\bullet_{Me}] = [p'_{Me}], \tag{6b}$$

and

$$[p^\bullet] = [p'_{Me}]. \tag{6c}$$

Here, the notation p'_{Me} is shorthand for a defect associate formed between a proton and a metal vacancy, $p'_{Me} \equiv \{p^\bullet - V''_{Me}\}'$. Note that O–H stretching bands in infrared spectra indicate that protons (hydrogen ions) are physically located in the electron cloud of the oxygen ions; also note that an unassociated proton is equivalent to an interstitial hydrogen ion, $p^\bullet \equiv H^\bullet_i$. Reactions can be written for the two defects in each of the three charge neutrality conditions given in Eq. 6. For example, for the charge neutrality condition given by Eq. 6c, the corresponding reaction equation is

$$\begin{aligned} H_2O + Me^\times_{Me} &\Leftrightarrow H^\bullet_i + H'_{Me} + MeO(srg) \\ &\equiv p^\bullet + p'_{Me} + MeO(srg). \end{aligned} \tag{7}$$

If the law of mass action is applied to Eq. 7 and the result is combined with Eq. 6c, then

$$[p^\bullet] = [p'_{Me}] \propto f^{1/2}_{H_2O}\, a^{-1/2}_{MeO}. \tag{8}$$

As will become clear in the discussion below, a second important defect associate involving protons and cation vacancies is

$$(2p)^\times_{Me} \equiv \{2p^\bullet - V''_{Me}\}^\times. \tag{9}$$

These defect associates form via the reaction

$$H_2O + Me^\times_{Me} \Leftrightarrow \{2p^\bullet - V''_{Me}\}^\times + MeO(srg). \tag{10}$$

The law of mass action applied to reaction (10) yields

$$[\{2p^\bullet - V''_{Me}\}^\times] \propto f^0_{O_2} f^1_{H_2O}\, a^1_{MeO}\, x^0. \tag{11}$$

The total concentration of cation vacancies can now be written as

$$[V^{tot}_{Me}] = [V''_{Me}] + [\{p^\bullet - V''_{Me}\}'] + [\{2p^\bullet - V''_{Me}\}^\times]. \tag{12}$$

Since protons diffuse rapidly compared to metal vacancies, all these vacancies contribute to cation diffusion. Hence, the presence of protons will directly enhance the rate of cation interdiffusion, which can be expressed as [33]

$$\tilde{D}_{Fe-Mg} = X^{tot}_{V_{Me}} \tilde{D}_{V_{Me}}, \tag{13}$$

where $\tilde{D}_{Fe-Mg}$ is the Fe–Mg interdiffusion coefficient, $X^{tot}_{V_{Me}} \equiv [V^{tot}_{Me}]$, and $\tilde{D}_{V_{Me}}$ is the effective cation vacancy diffusivity, which is generally well approximated to be independent of the concentration of vacancies for dilute vacancy concentrations [34, p. 67].

In the application of such analyses to processes in the deep interior of Earth, a significant range of fluid pressures may be appropriate, up to ~130 GPa, the pressure at the core-mantle boundary. As can be seen from Fig. 1, water fugacity increases rapidly with increasing fluid pressure above ~1 GPa, strongly favoring the presence of hydrous defects at high pressures. Therefore, water fugacity is a particularly important thermodynamic parameter in investigations of the role of protons on diffusion kinetics.

Data analysis

(Mg, Fe)O

Recent experimental results on Fe–Mg interdiffusion in the $(Mg_{1-x}Fe_x)O$ system revealed a small but persistent

Table 1 Dependencies of point defect concentrations in (Mg, Fe)$_2SiO_4$ on oxygen fugacity, water fugacity, activity of enstatite, and mole fraction of iron for four possible charge neutrality conditions, expressed as the exponents m, n, q, and r, in the relationship $[\ ] \propto f^m_{O_2} f^n_{H_2O}\, a^q_{MeO}\, x^r$ (the same dependencies hold for (Mg, Fe)O except that $q = 0$)

Charge neutrality	$[Fe^\bullet_{Me}]$	$[V''_{Me}]$	$[H^\bullet_i]$	$[H'_{Me}]$	$[(2H)^\times_{Me}]$
$[Fe^\bullet_{Me}] = 2[V''_{Me}]$	$\frac{1}{6}\ 0\ \frac{-1}{3}\ \frac{2}{3}$	$\frac{1}{6}\ 0\ \frac{-1}{3}\ \frac{2}{3}$	$\frac{-1}{12}\ \frac{1}{2}\ \frac{-1}{3}\ \frac{-1}{3}$	$\frac{1}{12}\ \frac{1}{2}\ \frac{-2}{3}\ \frac{1}{3}$	01−10
$[Fe^\bullet_{Me}] = [H'_{Me}]$	$\frac{1}{8}\ \frac{1}{4}\ \frac{-1}{2}\ \frac{1}{2}$	$\frac{1}{4}\ \frac{-1}{2}\ 0\ 1$	$\frac{-1}{8}\ \frac{3}{4}\ \frac{-1}{2}\ \frac{-1}{2}$	$\frac{1}{8}\ \frac{1}{4}\ \frac{-1}{2}\ \frac{1}{2}$	01−10
$[H^\bullet_i] = 2[V''_{Me}]$	$\frac{1}{4}\ \frac{-1}{6}\ \frac{-1}{3}\ 1$	$0\ \frac{1}{3}\ \frac{-1}{3}\ 0$	$0\ \frac{1}{3}\ \frac{-1}{3}\ 0$	$0\ \frac{2}{3}\ \frac{-2}{3}\ 0$	01−10
$[H^\bullet_i] = [H'_{Me}]$	$\frac{1}{4}\ 0\ \frac{-1}{2}\ 1$	0 0 0 0	$0\ \frac{1}{2}\ \frac{-1}{2}\ 0$	$0\ \frac{1}{2}\ \frac{-1}{2}\ 0$	01−10

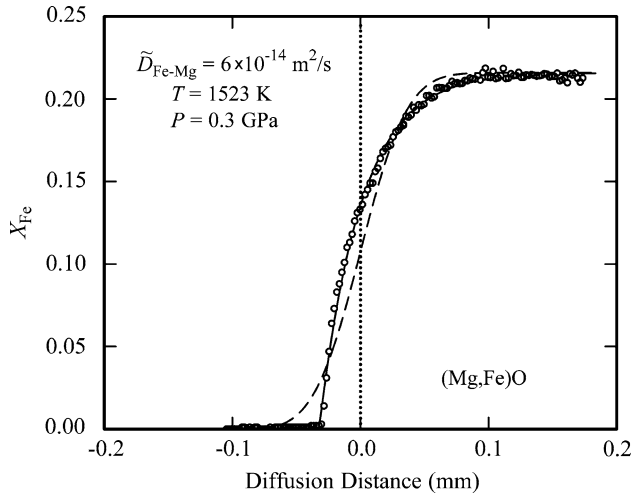

Fig. 2 Plot of Fe concentration versus diffusion distance for a diffusion couple composed of single crystals of MgO and $(Mg_{0.78}Fe_{0.22})O$ [21]. The Boltzmann–Matano interface is marked by the vertical dotted line at a diffusion distance of 0 mm. The solid curve is a least squares fit of the data to Eq. 14, while the dashed curve is a fit of the data to Eq. 15. The diffusion experiment was carried out under water-saturated conditions for 2 h at the P, T conditions indicated in the figure

increase in interdiffusivity in samples annealed in a hydrothermal environment compared to samples annealed under anhydrous conditions [21]. One diffusion profile is plotted in Fig. 2. To determine the interdiffusivity as a function of composition based on a Boltzmann–Matano analysis [e.g., 34, p. 87, 35], these data were fit to the equation

$$X_{Fe}(z) = B_0\left(1 - \frac{1}{(1+\exp(B_1 z + B_2))^{B_3}}\right) \quad (14)$$

where $X_{Fe} \equiv x$ is mole fraction of Fe; z is diffusion distance; and B_0, B_1, B_2, and B_3 are fitting parameters. To illustrate the dependence of diffusivity on Fe concentration, the diffusion profile was also fit to the relation for diffusion with a concentration-independent diffusivity, D, for comparison:

$$X_{Fe}(z) = -C_0/2\mathrm{erfc}(z/2\sqrt{Dt}) + C_1, \quad (15)$$

where t is the duration of the diffusion anneal; the parameters C_0 and C_1 are determined from a nonlinear least squares regression to the data. A strong dependence of $\tilde{D}_{Fe-Mg}$ on Fe concentration is clearly indicated.

In experiments performed under hydrous conditions, Demouchy et al. [21] jacketed their samples in Ni such that oxygen fugacity was buffered by the Ni/NiO solid-state reaction. In analyzing their data, these authors did not consider an oxygen fugacity dependence of the interdiffusion coefficients, despite the earlier determination that $\tilde{D}_{Fe-Mg} \propto f_{O_2}^{1/6}$ for anhydrous interdiffusion [36]. It is noteworthy that oxygen partial pressure is a function of temperature, increasing from 6×10^{-6} to 8×10^{-3} Pa at the Ni/NiO solid-state reaction as temperature is increased from 1,000 to 1,250°C [8], the range of temperatures used in the Demouchy et al. [21] interdiffusion experiments. Thus, any dependence of interdiffusivity on oxygen fugacity is absorbed in the activation energy for diffusion.

In reanalyzing the hydrous interdiffusion data, we considered several possible charge neutrality conditions (Table 1) as well as possible predominance of interdiffusion by unassociated metal vacancies, defect associates of a single proton and a metal vacancy, p'_{Me}, and defect associates of two protons and a metal vacancy, $(2p)^{\times}_{Me}$. For the same charge neutrality condition as in the anhydrous interdiffusion studies, Eq. 2, unassociated metal vacancies must, by definition, predominate; in this case, there is no internally consistent way to explain the significantly faster interdiffusion observed under hydrous conditions. For any charge neutrality condition for which $(2p)^{\times}_{Me}$ defects provide the majority of the cation vacancies for interdiffusion, no dependence on iron concentration is predicted, a situation that is inconsistent with the experimental results. Thus, as with Demouchy et al. [21], we have identified the likely predominant source of cation vacancies as the defect associate p'_{Me} with the likely charge neutrality condition given by Eq. 6b, $[Fe^{\bullet}_{Me}] = [p'_{Me}]$. In this case, we would anticipate oxygen fugacity and water fugacity exponents for interdiffusion of 1/8 and 1/4, respectively. Therefore, we normalized the interdiffusion data of Demouchy et al. [21] to a common oxygen fugacity and a common water

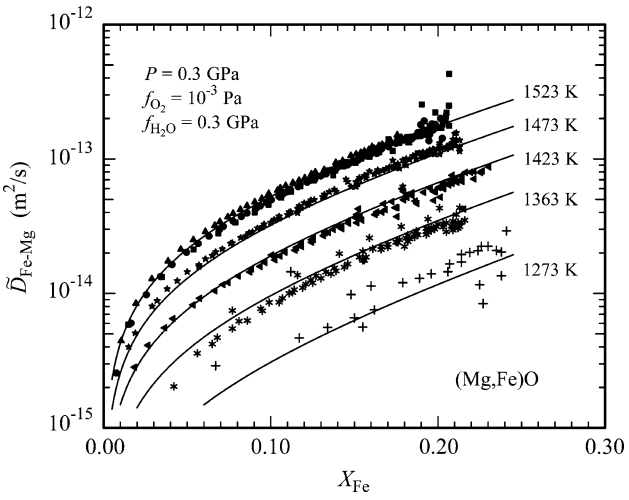

Fig. 3 Plot of Fe–Mg interdiffusivity versus iron concentration for diffusion couples formed between single crystals of MgO and $(Mg_{0.78}Fe_{0.22})O$ annealed at several temperatures and P = 0.3 GPa under water-saturated conditions. Data were normalized to the water fugacity and oxygen fugacity given in the figure, as described in the text. The conditions for each diffusion anneal are listed in Table 1 of Demouchy et al. [21]

fugacity using the relation $\tilde{D}_{\mathrm{Fe-Mg}} \propto f_{\mathrm{O_2}}^{1/8} f_{\mathrm{H_2O}}^{1/4}$ and plotted the resulting interdiffusivity as a function of Fe concentration in Fig. 3 for several annealing temperatures. The normalized data for hydrous interdiffusion at all five experimental temperatures were fit to the relation [37–41, p. 38]

$$\tilde{D}_{\mathrm{Fe-Mg}} = \tilde{D}_0 f_{\mathrm{O_2}}^m f_{\mathrm{H_2O}}^n x^r \exp[-(Q + \alpha x)/RT] \quad (16)$$

yielding $r = 0.85 \pm 0.04$, $Q = 208 \pm 2$ kJ/mol, and $\alpha = -79 \pm 4$ kJ/mol. By comparison, analysis of the interdiffusion profiles obtained from experiments carried out under anhydrous conditions ($n = 0$) give $m = 0.19 \pm 0.01$, $r = 0.73 \pm 0.03$, $Q = 209 \pm 7$ kJ/mol, and $\alpha = -96 \pm 5$ kJ/mol [36]. It is worth noting that the value of $r = 0.85$ for hydrous interdiffusion is significantly larger than the value predicted by the point defect model of $r = 0.5$ given in Table 1 for the charge neutrality condition $[\mathrm{Fe}_{\mathrm{Me}}^{\bullet}] = [\mathrm{p}'_{\mathrm{Me}}]$ and the defect associate $\mathrm{p}'_{\mathrm{Me}}$ as the dominant source of cation vacancies. A value of $r > 0.5$ is clearly supported by the data but may result from the transition in control of diffusion from unassociated vacancies, $\mathrm{V}''_{\mathrm{Me}}$, for which $r = 1.0$, to proton-vacancy associates, $\mathrm{p}'_{\mathrm{Me}}$. The uncertainties quoted above for hydrous and anhydrous conditions represent the 1σ errors calculated from the nonlinear least squares regression fits of all parameters to all (hydrous or anhydrous) data. As such, they do not adequately reflect the uncertainties in experimental temperature (and hence oxygen fugacity), duration, and analytical error. Thus, these values underestimate the true uncertainties in the parameters.

$(Mg, Fe)_2SiO_4$

Recent experimental results on Fe–Mg interdiffusion in the $(Mg_{1-x}Fe_x)_2SiO_4$ system revealed an approximately linear dependence of interdiffusivity on water fugacity with $n = 0.9 \pm 0.3$ [22, 23]. However, these authors did not quantify the dependence of interdiffusivity on Fe concentration. One of the diffusion profiles from Wang et al. [22] is plotted in Fig. 4, along with least squares fits to Eqs. 14 and 15. A comparison of the two fits suggests that interdiffusivity is at least weakly dependent on Fe concentration.

The diffusion profile in Fig. 4 was fit to Eq. 16, yielding interdiffusivity as a function of Fe concentration plotted in Fig. 5. Two features differ from those in Fig. 3 for (Mg, Fe)O. First, the data lie on a straight line indicating that $r = 0$ in Eq. 16. This result, combined with the linear dependence of interdiffusivity on water fugacity, indicates that under hydrous conditions the predominant diffusing Me defects in $(Mg, Fe)_2SiO_4$ are the vacancies in the defect associates $(2p)_{\mathrm{Me}}^{\times}$ (see Table 1). Second, $\tilde{D}_{\mathrm{Fe-Mg}}$ decreases with increasing Fe concentration, yielding

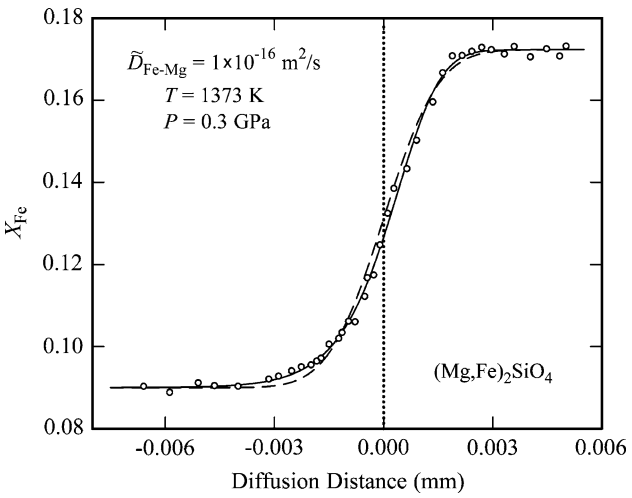

Fig. 4 Plot of Fe concentration versus diffusion distance for a diffusion couple composed of single crystals of $(Mg_{0.91}Fe_{0.09})_2SiO_4$ and $(Mg_{0.83}Fe_{0.17})_2SiO_4$ [22]. The Boltzmann–Matano interface is marked by the vertical dotted line at a diffusion distance of 0 mm. The solid curve is a least squares fit of the data to Eq. 14, while the dashed curve is a fit of the data to Eq. 15. The diffusion experiment was carried out under water saturated conditions for 2 h at the P, T conditions indicated in the figure

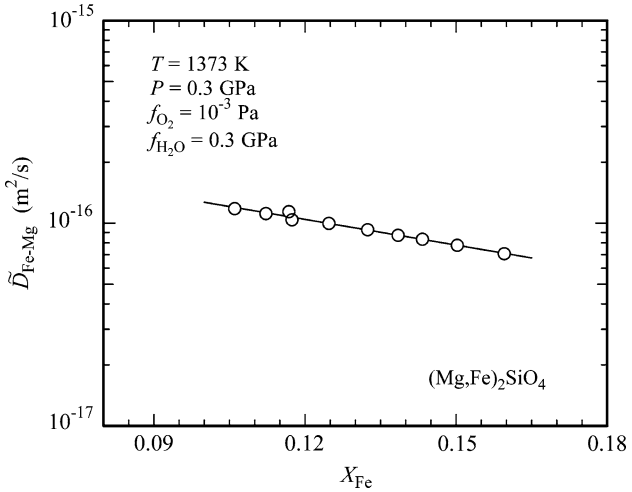

Fig. 5 Plot of Fe–Mg interdiffusivity versus iron concentration for diffusion couples formed between single crystals of $(Mg_{0.91}Fe_{0.09})_2SiO_4$ and $(Mg_{0.83}Fe_{0.17})_2SiO_4$ annealed at the conditions indicated in the figure

$\alpha = 110 \pm 5$ kJ/mol, opposite in sign to the results reported for (Mg, Fe)O under both anhydrous and hydrous conditions [21, 36] and for $(Mg, Fe)_2SiO_4$ under anhydrous conditions [31, 33]. Although the interdiffusion data do not constrain the charge neutrality condition since all charge neutrality conditions yield $\tilde{D}_{\mathrm{Fe-Mg}} \propto [(2p)_{\mathrm{Me}}^{\times}] \propto f_{\mathrm{H_2O}}^1 x^0$ (Table 1), it is most likely set by the relation in Eq. 6c, $[\mathrm{p}^{\bullet}] = [\mathrm{p}'_{\mathrm{Me}}]$.

Discussion

Under hydrous conditions, the Fe–Mg interdiffusivity for the (Mg, Fe)O system can be described by Eq. 16 as

$$\tilde{D}_{\mathrm{Fe-Mg}} = 2.9 \times 10^{-6} f_{\mathrm{O_2}}^{1/8} f_{\mathrm{H_2O}}^{1/4} x^{0.85} \times \exp[-(208000 - 79000x)/RT]\,(\mathrm{m^2/s}) \quad (17)$$

with $f_{\mathrm{O_2}}$ in Pa and $f_{\mathrm{H_2O}}$ in GPa. The comparison of this Fe–Mg interdiffusivity with the interdiffusivity obtained under anhydrous conditions in Fig. 6 illustrates that, at $P = 0.3$ GPa for which $f_{\mathrm{H_2O}} \approx 0.3$ GPa, protons have only a modest effect on diffusion. Over the range of Fe concentrations explored experimentally, interdiffusion is consistently a factor of 3 faster under hydrous conditions than under anhydrous conditions. Yet, the dependencies on temperature (activation energy) and on Fe concentration are identical within experimental uncertainty. These observations suggest that the vacancy concentration is increased when protons are introduced into the samples resulting in a change in charge neutrality condition, where the predominant negative defect is now a proton-vacancy associate, p'_{Me}, as given in Eq. 6b. These defect associates dominate diffusion, as described in Eq. 12, and are responsible for the enhanced rate of diffusion.

Under hydrous conditions, the Fe–Mg interdiffusivity for the (Mg, Fe)$_2$SiO$_4$ system is controlled by diffusion of $(2p)^{\times}_{\mathrm{Me}}$. The Fe–Mg interdiffusivity can be described by Eq. 16 as

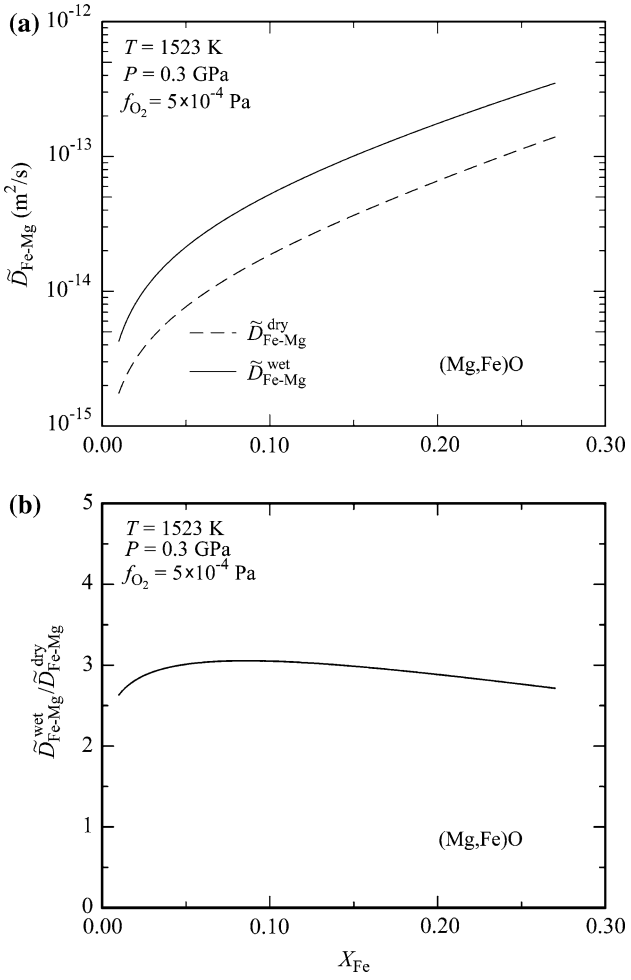

Fig. 6 (**a**) Comparison of Fe–Mg interdiffusivity versus iron concentration for experiments carried out under wet (hydrous) and dry (anhydrous) conditions for the (Mg, Fe)O system. (**b**) Ratio of Fe–Mg interdiffusivity determined under hydrous conditions with that determined under anhydrous conditions versus iron concentration. Note that the ratio of interdiffusivities is ~3, independent of iron concentration

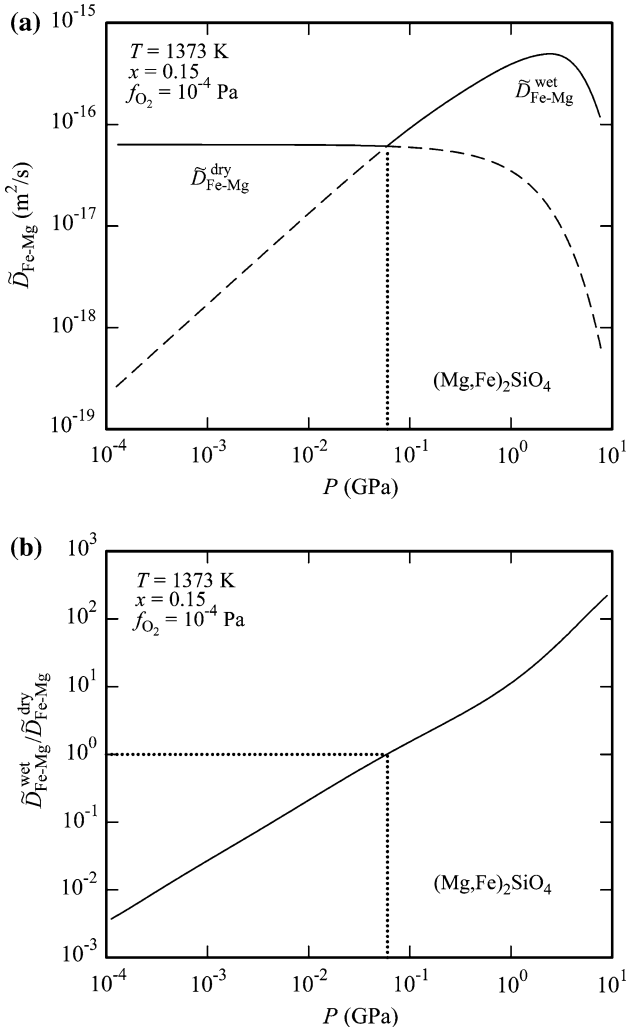

Fig. 7 (**a**) Comparison of Fe–Mg interdiffusivity versus pressure for experiments carried out under wet (hydrous) and dry (anhydrous) conditions for the (Mg, Fe)$_2$SiO$_4$ system. (**b**) Ratio of Fe–Mg interdiffusivity determined under hydrous conditions with that determined under anhydrous conditions versus pressure. Note that for $P > 60$ MPa diffusion under hydrous conditions occurs more rapidly than diffusion under anhydrous conditions. This transition pressure corresponds to $f_{\mathrm{H_2O}} \approx 60$ MPa

$$\tilde{D}_{\mathrm{Fe-Mg}} = 3 \times 10^{-8} f_{\mathrm{O_2}}^{0} f_{\mathrm{H_2O}}^{1} a_{\mathrm{MeO}}^{1} x^{0} \times \exp[-(205000 + 16 \times 10^{-6} P + 110000x)/RT] (\mathrm{m^2/s}) \quad (18)$$

with f_{H_2O} in GPa, P in Pa, and activation volume for diffusion of 16×10^{-6} m^3/mol. The comparison of this Fe-Mg interdiffusivity with the interdiffusivity obtained under anhydrous conditions in Fig. 7 illustrates that protons have a substantial effect for $f_{H_2O} > 0.1$ GPa. A switch from interdiffusion governed by anhydrous to hydrous behavior occurs at $f_{H_2O} \approx 60$ MPa, in good agreement with the value of $f_{H_2O} \approx 50$ MPa determined in both diffusion and dislocation creep experiments on olivine [15, 16]. The proton concentration at $f_{H_2O} \approx 60$ MPa is ~ 120 H/10^6 Si or a concentration of $(2p)_{Me}^{\times}$ defects of ~ 60 at. ppm [42, 43]. This vacancy concentration is similar to the value of ~ 70 at. ppm, determined from thermogravimetric measurements under anhydrous conditions [31, 44].

For both materials, the rate of interdiffusion under hydrous conditions increases significantly with increasing water fugacity. This response reflects both a change in the defect species that define charge neutrality and in the nature of the diffusing point defect species. With increasing hydrogen concentration, the mechanism of cation interdiffusion changes from one dominated by unassociated metal vacancies, V''_{Me}, to one controlled by defect associates formed between a single proton and a metal vacancy, $\{p^{\bullet} - V''_{Me}\}'$, to one controlled by defect associates formed between two protons with a metal vacancy, $\{2p^{\bullet} - V''_{Me}\}^{\times}$. The concentration of this last defect increases linearly with increasing water fugacity. Protons from these defects expected to dominate electrical conductivity under deep Earth conditions. Thus, with the strong dependence of water fugacity on fluid pressure illustrated in Fig. 1, conductivity profiles of Earth's interior provide a technique for probing the water content as a function of depth.

Conclusion

Interdiffusion of Fe and Mg in iron–magnesium oxides and silicates is enhanced in the presence of hydrogen. This enhancement results from an increase in the total concentration of metal vacancies in the materials through formation of proton-vacancy defect associates with increasing water fugacity. In the case of the iron–magnesium oxides the predominant defect associates at the conditions of our experiments involve a single proton associated with a metal vacancy, while in the silicates, the predominant defect associates involve 2 protons and a metal vacancy. These results predict that the presence of water dissolved in minerals in the deep Earth will significantly affect diffusion and associated kinetic processes, relative to kinetic behavior under dry conditions.

Acknowledgments Support from the National Science Foundation through grants EAR-0439747 (DLK) and EAR-0337012 (SJM) is gratefully acknowledged. The authors thank Dr. Sylvie Demouchy for her help. This article is LPI publication #1381.

References

1. Kohlstedt DL (2006) Water in nominally anhydrous minerals. Rev Mineral Geochem, vol 62, Mineralogical Society of America, p 377
2. Kohlstedt DL (2007) Treatise on geophysics, vol 2.14. Elsevier Ltd, Oxford, p 389
3. Karato S-I (2006) Earth's deep water cycle. Geophys Monogr 168:113. Amer Geophys Union, Washington DC
4. Griggs DT, Blacic JD (1965) Science 147:292
5. Blacic JD (1972) Flow and fracture of rocks. Amer Geophys Union, Washington DC, p 109
6. Mackwell SJ, Kohlstedt DL, Paterson MS (1985) J Geophys Res 90:11319
7. Karato S-I (1989) Rheology of solids and of the earth. Oxford University Press, Oxford, p 176
8. Mackwell SJ, Kohlstedt DL (1990) J Geophys Res 95:5079
9. Kohlstedt DL, Mackwell SJ (1998) Zeitschrift für Physikalische Chemie 207:147
10. Tullis J, Yund RA (1980) J Struct Geol 2:439
11. Bystricky M, Mackwell S (2001) J Geophys Res 106:13433
12. Hier-Majumder S, Mei S, Kohlstedt DL (2005) J Geophys Res 110:B07406. doi:10.1029/2004JB003414
13. Kohlstedt DL, Evans B, Mackwell SJ (1995) J Geophys Res 100:17587
14. Post AD, Tullis J, Yund RA (1996) J Geophys Res 101:22143
15. Mei S, Kohlstedt DL (2000) J Geophys Res 105:21457
16. Mei S, Kohlstedt DL (2000) J Geophys Res 105:21471
17. Mei S, Bai W, Hiraga T, Kohlstedt DL (2002) Earth Planet Sci Lett 201:491
18. Hirth G, Kohlstedt DL (2003) Inside the subduction factory. Geophys Monogr 138:83. Amer Geophys Union, Washington, DC
19. Karato S-I, Jung H (2003) Philos Mag 83:401
20. Chen S, Hiraga T, Kohlstedt DL (2006) J Geophys Res 111. doi:10.1029/2005JB003885
21. Demouchy S, Mackwell SJ, Kohlstedt DL (2007) Contrib Mineral Petrol. doi:10.1007/s00410-007-0193-9
22. Wang Z, Hiraga T, Kohlstedt DL (2004) Appl Phys Lett 85:209
23. Hier-Majumder S, Anderson IM, Kohlstedt DL (2005) J Geophys Res 110:B02202. doi:10.1029/2004JB003292
24. Costa F, Chakraborty S (2008) Phys Earth Planet Inter 166:11. doi:10.1016/jpepi.2007.10.006
25. Huang X, Xu Y, Karato S (2005) Nature 434:746
26. Wang D, Mookherjee M, Xu Y, Karato S (2006) Nature 443:977
27. Yoshino T, Matsuzaki T, Yamashita S, Katsura T (2006) Nature 443:973
28. Pitzer KS, Sterner SM (1994) J Chem Phys 101:3111
29. Valet P-M, Plushkell W, Engell H-J (1975) Arch Eisenhuettenwes 46:383
30. Gourdin WH, Kingery WD (1979) J Mater Sci 14:2053
31. Dohmen R, Chakraborty S (2007) Phys Chem Minerals 34. doi:10.1007/s00269-007-0158-6
32. Kröger FA, Vink HJ (1956) Solid state physics, vol 3. Academic Press, San Diego, CA, p 307
33. Nakamura A, Schmalzried H (1984) Ber Bunsenges Phys Chem 88:140

34. Schmalzried H (1981) Solid state reactions. Elsevier, New York
35. Matano C (1933) Japan J Phys 8:109
36. Mackwell SJ, Bystricky M, Sproni C (2005) Phys Chem Minerals. doi:10.1007/s00269-005-0013-6
37. Schwier VG, Dieckmann R, Schmalzried H (1973) Ber Bunsenges Phys Chem 77:402
38. Dieckmann R, Schmalzried H (1975) Ber Bunsenges Phys Chem 70:1108
39. Nakamura A, Schmalzried H (1983) Phys Chem Minerals 10:27
40. Morioka M (1989) Rheology of solids and of the earth. Oxford University Press, Oxford, p 156
41. Schmalzried H (1995) Chemical kinetics of solids. VCH Verlagsgesellschaft, Weinheim
42. Bai Q, Kohlstedt DL (1992) Nature 357:672
43. Kohlstedt DL, Keppler H, Rubie DC (1996) Contrib Mineral Petrol 123:345
44. Tsai T-L, Dieckmann R (2002) Phys Chem Minerals 29:680